ELSEVIER

European Polymer Journal 36 (2000) 1607–1611

EUROPEAN POLYMER JOURNAL

A Monte Carlo study of polymer network dynamics

Linxi Zhang[a,*], Yun Xu[a], Delu Zhao[b]

[a]Department of Physics, Zhejiang University, Hangzhou 310028, People's Republic of China
[b]Institute of Chemistry, Chinese Academy of Sciences, Beijing 100080, People's Republic of China

Received 13 April 1999; received in revised form 12 July 1999; accepted 18 August 1999

Abstract

Junction fluctuations in a polymer network are investigated by using the Monte Carlo method. In our calculation, a modified bond-fluctuation model is adopted. In our model, the kuhnian bond lengths are set to vary between 2 and 4, which is different from the lengths between 2 and $\sqrt{10}$ of the standard model. It is found that the average fluctuations of junctions i and j may be expressed in the form of

$$\langle \Delta R_i^2 \rangle / \langle r^2 \rangle_0 = \frac{a}{(\phi - 1)} + b(\phi = 3, 4, 5, 6)$$

$$\langle \Delta R_i \Delta R_j \rangle / \langle r^2 \rangle_0 = \frac{a'}{(\phi - 1)} + b'(\phi = 3, 4, 5, 6)$$

where $a = 0.83$, $b = -0.076$, $a' = 0.06$, $b' = 0.0075$, and $\langle r^2 \rangle_0$ is the mean-square end-to-end distance of two adjacent junction points and ϕ is the junction functionality. Comparisons with the Cayley tree model are also made. Our method uses real, rather than phantom, chains, and this method can be used to investigate the dynamics of polymer network chains.

1. Introduction

The phantom network model of networks forms the basis of some theories of rubber elasticity [1]. The mathematical structure of the model was first outlined in detail by James [2] and James and Guth [3]. It is based on assumptions describing the transformations of junction points under macroscopic deformation. Junctions are joined by Gaussian chains which may pass freely through one another as they undergo rapid fluctuations according to the kinetic characteristic of polymeric media. The importance of the model in interpreting molecular deformation, neutron scattering and effects of entanglements were realized much later [4–8].

The first systematic treatment of junction fluctuations for interpreting scattering from deformed phantom networks was given by Pearson [5]. A concise and complete deviation of junction fluctuations in phantom networks was given by Kloczkowski et al. for unimodal and bimodal networks having the topology of a Cayley tree [6]. In a Cayley tree (see Fig. 1), there is no randomness, and there are no loops. Chains originating from junctions of the ith tier terminate in junctions of the $(i + 1)$th tier, and the junctions on the final tier are assumed to be fixed in space. They are considered only as networks that have a treelike structure and symmetrically grow about a central chain. This model is not an entirely realistic one. In a real network, the operational definition of a tier becomes

* Corresponding author.

0014-3057/00/$ - see front matter
PII: S0014-3057(99)00220-7

ambiguous and there is no a central chain. In the present study, we attempt to give the configurations of the real polymer networks using the Monte Carlo method.

2. Simulation method

As polymers are very complicated topological objects, computer simulation is always the best tool to get precise theoretical information on the proposed model. The standard algorithms do not allow for the simulation of the two-dimensional polymers and branched objects. Branching points cannot move. The standard algorithms might cause difficulties for very dense systems. An effective algorithm, the bond-fluctuation model, was developed by Carmesin and Kremer [9], and this method was widely applied to the investigation of dynamics of complicated systems [10–14]. This method can also be used to investigate the configurational properties of complicated systems. In the bond-fluctuation model, the monomers are connected by bond vectors whose lengths are set to vary between 2 and $\sqrt{10}$ in three dimensions. Using these restrictions on the bond lengths, six basic classes of bond vectors can be constructed, allowing 108 different bond vectors and 87 bond angles. The basic bonds are (2, 0, 0), (2, 1, 0), (2, 1, 1), (2, 2, 1), (3, 0, 0), and (3, 1, 0) [10]. We notice that the functionality ϕ in the polymer network may have a large value. If the bond-fluctuation model is adopted, the junction points with a large functionality cannot move. The reason is that the bond (Kuhnian bond) length in the bond-fluctuation model is only between 2 and $\sqrt{10}$. After the movement, some new bond lengths may become shorter than 2, or longer than $\sqrt{10}$ and the junction points always remains at their original positions. Therefore, in our simulation, a modified bond-fluctuation model should be adopted. In our modified bond-fluctuation model, the bond lengths are set to vary between 2 and 4, and the number of allowed bond vectors is greater than 108. In fact, the bond-fluctuation model exploits this idea of the Kuhnian bond and translates it onto a lattice [9,15]. The properties of these Kuhnian bonds depend upon the number of chemical monomers in the effective beads. The number of chemical monomers may be 4, or 5, or 6, or 7, or even more. Therefore, the Kuhnian bond may have a large range of bond lengths.

In our simulation, the model of James is also considered. In the method of James it is assumed that the network is connected to a set of fixed points which lie on the bounding surface of the material. These points preserve the volume of the network and move affinely with the dimensions of the sample on deformation. In the method of Deam and Edwards [16] the additional constraint is imposed by assuming that the density is constant throughout the network. If the box size is $L \times L \times L$, the number of junction points is L^3. At the beginning, the distances between two adjacent junction points are the same (equal to $\mathbf{r}_0$) for all junction points and the junction points in the network have equal functionality ϕ. Fig. 2 shows the starting configuration of the 5-functional polymer network with the network size of $1 \times 1 \times 1$. This means that the number of junction points is 1. Here the polymer points on the bounding surface are fixed and are not included. Two adjacent junction points are connected with a chain. If the functionality $\phi < 6$, the chain connected to two adjacent junctions is chosen at random. Then the junction points move according to the following algorithm. To move the point, a junction point is selected at random. Then it tries to jump at random with the distance of unity into one of the six possible lattice directions. If the move complies with the Kuhnian bond length restriction, it is accepted and the cycle is terminated. If not, a new junction point is selected at random, and so on. Here the new junction position should be checked. If the new position is occupied, the junction point remains at its original position and the cycle is terminated. After being created, the polymer network is

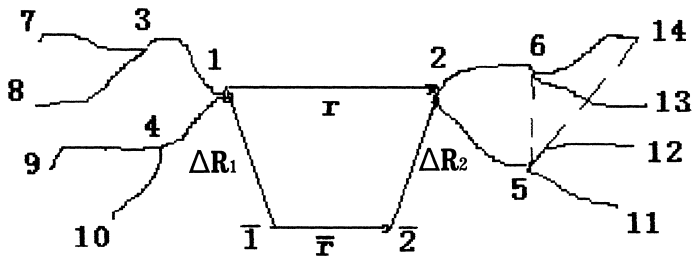

Fig. 1. First three tiers of the symmetrically grown trifunctional ($\phi = 3$) network with a treelike structure. Points 1 and 2 denote ends of the chain at the given instant and $\bar{1}$ and $\bar{2}$ their mean time-averaged positions. ΔR_1 and ΔR_2 are instantaneous fluctuations of points 1 and 2 from their mean positions.

relaxed for at least 1.0×10^4 MCS. One Monte Carlo step (1 MCS) is one attempted jump per junction point. After reaching equilibrium, the measurements are performed in intervals of 2500 MCS for an amount of 5.0×10^5 MCS. In order to improve the statistics, 100 independent configurations of this system were run.

3. Results and discussion

The instantaneous configuration in a network is shown in Fig. 1. Points 1 and 2 denote the ends of the chain at the instant. $\bar{r}$ is the time-averaged end-to-end vector and r is the instantaneous end-to-end vector. In Fig. 1, the first tier of polymer network is made up of the two junctions numbered from 1 to 2 and the second tier consists of the remaining 4 junctions labeled from 3 to 6. Eight junctions constitute the third tier. ΔR_1 and ΔR_2 are respectively the instantaneous fluctuations of the points 1 and 2 from their mean positions $\bar{1}$ and $\bar{2}$, and are defined by

$$\Delta R_1 = R_1 - \bar{R}_1$$

$$\Delta R_2 = R_2 - \bar{R}_2. \tag{1}$$

Time averages are designed by an overbar. Ensemble averages are denoted by an angular bracket.

For a polymer network, the equilibrium correlation between the fluctuations of junctions i and $j\langle\Delta\mathbf{R}_i\Delta\mathbf{R}_j\rangle$ is an important parameter. In Cayley trees of infinite size, the average fluctuations of junctions i and j separated by d other junctions along a path may be expressed by the matrix [6].

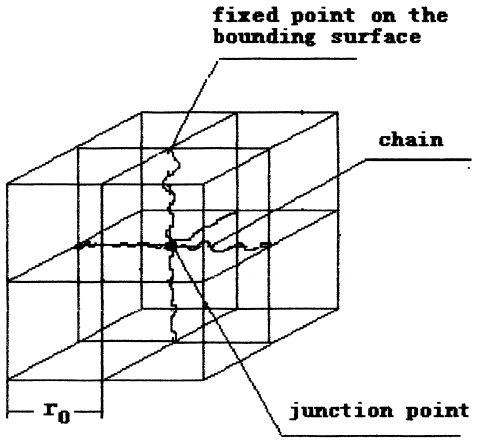

Fig. 2. The starting configuration of a 5-functional polymer network with the network size of $1 \times 1 \times 1$, here $\mathbf{r}_0 = 6$.

$$\begin{bmatrix} \langle \Delta\bar{R}_i^2 \rangle & \langle \Delta\bar{R}_i \Delta\bar{R}_j \rangle \\ \langle \Delta\bar{R}_i \Delta\bar{R}_j \rangle & \langle \Delta\bar{R}_j^2 \rangle \end{bmatrix} = \frac{3}{2\gamma} \begin{bmatrix} \dfrac{\phi-1}{\phi(\phi-2)} & \dfrac{1}{\phi(\phi-1)(\phi-2)^d} \\ \dfrac{1}{\phi(\phi-1)(\phi-2)^d} & \dfrac{\phi-1}{\phi(\phi-2)\phi} \end{bmatrix} \tag{2}$$

where ϕ is the junction functionality and $\gamma = 3/(2\langle r^2\rangle_0)$ ($\langle r^2\rangle_0$ is the unperturbed mean-square end-to-end distance of two adjacent junction points.) We notice that the Cayley tree is an approximate model. Chains always originate from junctions of the ith tier to junctions of the $(i + 1)$th tier and the junctions are not connected with each other in the same or the different tier. For example, in Fig. 1, junctions 5 and 6 in the same tier cannot be connected and junctions 5 and 14 in the different tier cannot be connected too in the Cayley tree model. In fact, the junctions can be connected to each other in the same tier or in the different one, and this leads the small values of the average fluctuations of junctions.

Fig. 3 displays the configurations at the different simulation time for the junction points of the second layer from the bounding surface. Here the junction functionality ϕ is 6 and the number of polymer network junction points is $5 \times 5 \times 5$ (the network size is $L = 5$). Fig. 3 show a slice of a 6-functional network in 3D as it is more difficult to show all junction positions clearly. The box length is $6\mathbf{r}_0$ and $\mathbf{r}_0$ equals 6 in the lattice spacing. The junction points on the bounding surface and of the third layer are not shown in Fig. 3. The initial state is shown in Fig. 3(a). After 20,000 MCS, the polymer network is in an equilibrium state. Fig. 3(b) is the configuration after 20,000 MCS and Fig. 3(c) after 40,000 MCS.

We first calculate the mean-square fluctuation of junction $i\langle\Delta R_i^2\rangle$ in the different network size, and the results are given in Fig. 4. Here $\langle\Delta R_i^2\rangle$ is the mean-square fluctuation from the time-averaged position and is averaged for all junction points. In Fig. 4, we find the ratios $\langle\Delta R_i^2\rangle/\langle r^2\rangle_0$ are almost the same junction functionality value. The ratio $\langle\Delta R_i^2\rangle/\langle r^2\rangle_0$ increases with a decrease in the junction functionality value ϕ. In order to investigate the relation between the ratio $\langle\Delta R_i^2\rangle/\langle r^2\rangle_0$ and the junction functionality ϕ in detail, we also plot the ratio $\langle\Delta R_i^2\rangle/\langle r^2\rangle_0$ as a function of $1/(\phi-1)$. The results are displayed in Fig. 5. We find the ratio $\langle\mathbf{R}_i^2\rangle/\langle r^2\rangle_0$ to have the form of

$$\langle\Delta R_i^2\rangle/\langle r^2\rangle_0 = \frac{a}{(\phi-1)} + b(\phi = 3, 4, 5, 6) \tag{3}$$

where $a = 0.83$ and $b = -0.076$ and the largest deviation from the Monte Carlo results is 4.5%. Although

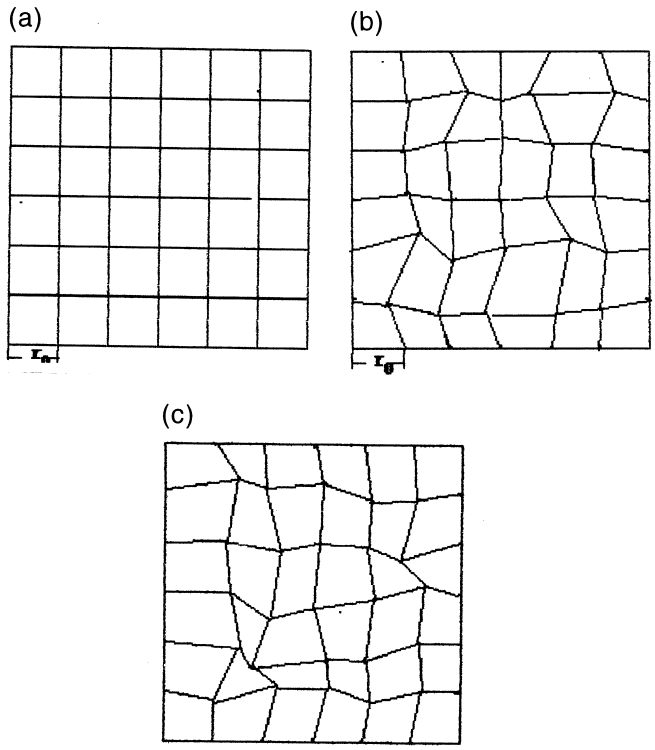

Fig. 3. Time evolution of a polymer network. (a) $T = 0$ MCS; (b) $T = 20{,}000$ MCS; (c) $T = 40{,}000$ MCS.

the values of a and b in Eq. (3) depend mainly on the simulation model, the relation between the ratio $\langle \Delta R_i^2 \rangle / \langle r^2 \rangle_0$ and the junction functionality ϕ is the same. We find that the ratio $\langle \Delta R_i^2 \rangle / \langle r^2 \rangle_0$ increases if in our modified bond-fluctuation model the possible bond lengths are set to vary between 2 and 6, etc. However, the ratio $\langle \Delta R_i^2 \rangle / \langle r^2 \rangle_0$ is also given in Eq. (3). Here the junction functionality ϕ only has four values. The reason is that the maximum functionality of simple cubic lattice is $\phi = 6$ (see Fig. 2). In the meantime, the ratio $\langle \Delta R_i^2 \rangle / \langle r^2 \rangle_0$ in our model is less than that in the Cayley tree model with the same junction functionality ϕ. For example, the ratio $\langle \Delta R_i^2 \rangle / \langle r^2 \rangle_0$ in our model is

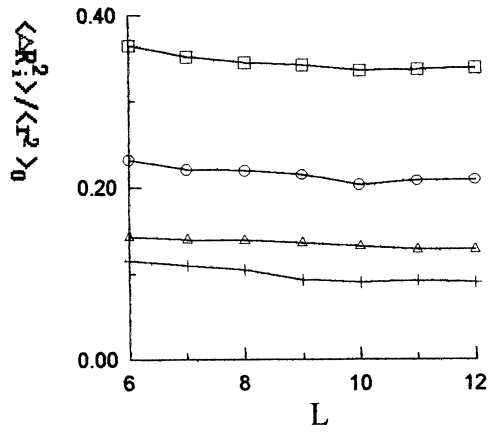

Fig. 4. The ratio $\langle \Delta R_i^2 \rangle / \langle r^2 \rangle_0$ vs network size L for polymer networks with four different junction functionality values. $\phi = 6$ (+); $\phi = 5$ (△); $\phi = 4$ (○) and $\phi = 3$ (□).

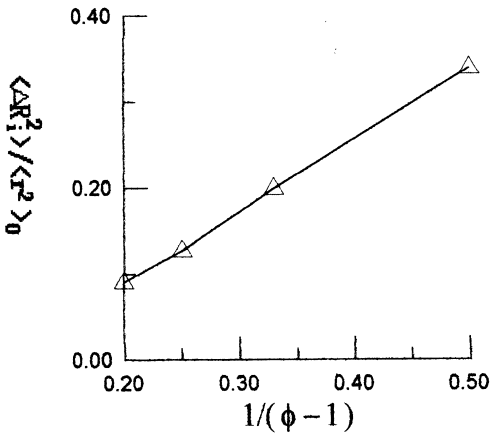

Fig. 5. The ratio $\langle \Delta R_i^2 \rangle / \langle r^2 \rangle_0$ vs $1/(\phi - 1)$.

0.339 for $\phi=3$ while it is 0.667 for $\phi=3$ in the Cayley tree model. In fact, the junction points move more easily in the Cayley tree model, and this leads to a larger fluctuation from its mean position. In addition, in the Cayley tree model, the ratio $\langle \Delta R_i^2\rangle/\langle r^2\rangle_0$ is

$$\langle \Delta R_i^2\rangle/\langle r^2\rangle_0 = \frac{\phi-1}{\phi(\phi-2)} \propto \frac{1}{\phi}, \tag{4}$$

and it is in direct proportion to the junction functionality ϕ. This relation is slightly similar to our results.

We also calculate the fluctuation $\langle \Delta \mathbf{R}_i \Delta \mathbf{R}_j\rangle$ of adjacent junction i and j, and the results are shown in Fig. 6. Similarly as $\langle \Delta \mathbf{R}_i^2\rangle$, the ratio $\langle \Delta \mathbf{R}_i \Delta \mathbf{R}_j\rangle/\langle r^2\rangle_0$ is also independent of the polymer network size L, and only depends on the junction functionality ϕ. In order to find the relationship between the ratio $\langle \Delta \mathbf{R}_i \Delta \mathbf{R}_j\rangle/\langle r^2\rangle_0$ and the junction functionality ϕ, we plot the ratio $\langle \Delta \mathbf{R}_i \Delta \mathbf{R}_j\rangle/\langle r^2\rangle_0$ vs $1/(\phi-1)$, and the results are displayed in Fig. 7. From Fig. 7, the expression can be obtained

$$\langle \Delta \mathbf{R}_i \Delta \mathbf{R}_j\rangle/\langle r^2\rangle_0 = \frac{a'}{(\phi-1)} + b'(\phi = 3,4,5,6) \tag{5}$$

where $a'=0.06$, $b'=0.0075$, and the standard deviation is less than 1.8%. Like for $\langle \Delta R_i^2\rangle$, our results are similarly smaller than that in the Cayley tree model.

In our model, as the maximum distance between two adjacent junction points is only $\mathbf{r}_0$ ($\mathbf{r}_0=6$), the maximum junction functionality ϕ is only $\phi=6$, and we here only study the configuration of a strained polymer network. If the distance of two adjacent junction points has a large range in the simulation model, we can pursue the statistic and dynamic properties of more complex polymer networks. This work is in progress.

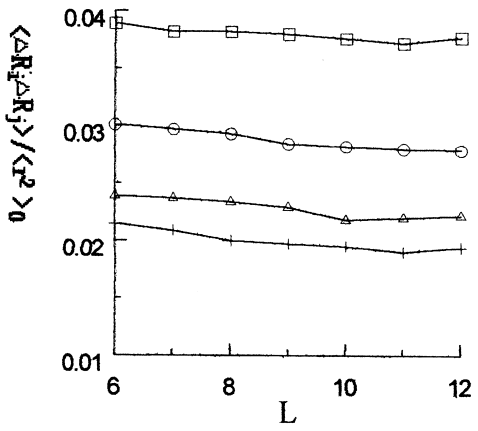

Fig. 6. The ratio $\langle \Delta R_i \Delta R_j\rangle/\langle r^2\rangle_0$ vs network size L for polymer networks with four different junction functionality values. $\phi=6$ (+); $\phi=5$ (△); $\phi=4$ (○) and $\phi=3$ (□).

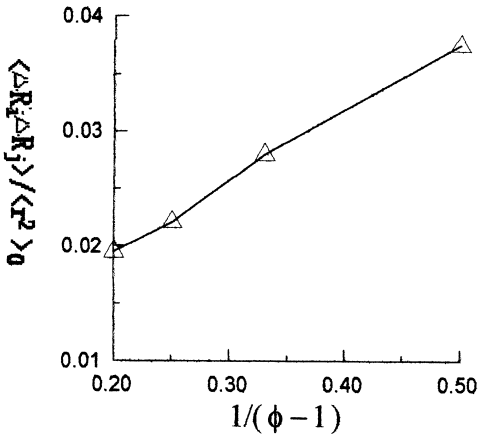

Fig. 7. The ratio $\langle \Delta R_i \Delta R_j\rangle/\langle r^2\rangle_0$ vs $1/(\phi-1)$.

Acknowledgements

This work was supported by the National Natural Science Foundation of China (No. 29874012) and The National Key Projects for Fundamental Research "Macromolecules Condensed State" from STCC.

References

[1] Erman B, Mark JE. Structure and properties of rubber-like network. Oxford: Oxford University Press, 1997.
[2] James HM. J Chem Phys 1947;15:651.
[3] James HM, Guth E. J Chem Phys 1953;21:1039.
[4] Flory PJ. Proc R Soc London A 1976;351:351.
[5] Pearson DS. Macromolecules 1977;10:696.
[6] Kloczkowski A, Mark JE, Erman B. Macromocules 1989;22:1423, 1992;25:2455.
[7] Graessley WW. Macromolecules 1977;13:272.
[8] Eichnger B. Ann Rev Phys Chem 1983;34:359.
[9] Carmesin I, Kremer K. Macromolecules 1988;21:2819.
[10] Baschnagel J, Binder K, Wittmann HP. J Phys C: Condensed Matter 1993;5:1597.
[11] Wittkop M, Kreitmeier S, Goritz D. J Chem Phys 1996;104:3373.
[12] Wittkop M, Kreitmeier S, Goritz D. Phys Rev E 1996;53:838.
[13] Zhang LX, Xia AG, Xu JM. J Chem Phys 1997;107:5582.
[14] Zhang LX, Xia AG, Xu JM, Zhao DL. Chin J Polym Sci, in press.
[15] Deutsch HP, Binder K. J Chem Phys 1991;94:2294.
[16] Deam RT, Edwards SF. Phil Trans R Soc London Ser A 1976;280:317.